Water Level Estimation and Reduction of Hydraulic Model Calibration Uncertainties Using Satellite SAR Images of Floods

ARTICLE *in* IEEE TRANSACTIONS ON GEOSCIENCE AND REMOTE SENSING · MARCH 2009

Impact Factor: 3.51 · DOI: 10.1109/TGRS.2008.2008718 · Source: IEEE Xplore

Water Level Estimation and Reduction of Hydraulic Model Calibration Uncertainties Using Satellite SAR Images of Floods

Renaud Hostache, Patrick Matgen, Guy Schumann, Christian Puech, Lucien Hoffmann, and Laurent Pfister

***Abstract*—Exploitation of river inundation satellite images, especially for operational applications, is mostly restricted to flood extent mapping. However, there lies significant potential for improvement in a 3-Dimensional characterization of floods (i.e. flood depth maps) and an integration of the Remote Sensing Derived (RSD) characteristics in hydraulic models. This study aims at developing SAR image analysis methods that go beyond flood extent mapping with a view to show the potential of these images in the spatio-temporal characterization of flood events. To meet this aim, two research issues were addressed. The first issue relates to water level estimation. The proposed method is composed of three steps: i) extraction of flood extent limits that are relevant for water level estimation, ii) water level estimation by merging relevant limits with a Digital Elevation Model, iii) constraining of the water level estimates using hydraulic coherence concepts. Applied to an ENVISAT image of an Alzette River flood (2003, Grand-Duchy of Luxembourg), this provides $\pm$ 54 cm average vertical uncertainty water levels, that were validated using a sample of ground surveyed high water marks. The second issue aims at better constraining hydraulic models using RSD water levels. To meet this aim, a "traditional" calibration using recorded hydrographs is completed via comparison between simulated and RSD water levels. This integration of the RSD characteristics proves to better constrain the model (i.e. the number of parameter sets providing acceptable results with respect to observations has been reduced) and render its forecasting more reliable.**

***Index Terms*—satellite SAR images, Digital Elevation Model, hydraulic coherence, hydraulic model calibration, uncertainty reduction.**

I. Introduction

IT is generally accepted that floods are among the most important natural hazard in the world. This explains the continuous efforts to better understand and manage them. To identify flood prone areas and to manage flood events, satellite images are believed to be very useful. Especially because of their all weather image acquisition capability, Synthetic Aperture Radar (SAR) satellites are very suitable for the spatial characterization of floods [1]. In this context, radar images of floods are nowadays mostly used for instantaneous flood extent extraction. Nevertheless, as mentioned by [2], there is no doubt that earth observation images contain information that goes beyond simple flood extents. Besides, hydraulic modeling is of paramount importance in most flood forecasting and management systems. Due to huge stakes in flood management, the reliability of these flood inundation models is of primary concern [3]. To be reliable, hydraulic models need to be constrained [4], for example during the calibration process, using various observed data sets. A model calibration generally consists in forcing the outputs of the model so as to be as close as possible to observed data, by modifying values of parameters. In an operational context, the calibration is often done using point observations, such as recorded hydrographs at hydrometric stations. However, these data are often insufficient to make the calibration reliable [5] as no reference data is available in the regions in-between these point measurements. According to [6]: "the apparent global optimal may change significantly with changes in calibration data, errors in input data or performance measure". This means that many values of parameters could allow the model to provide outputs close to observations and thus could be considered as acceptable with respect to observations. This has been introduced by [6] as the equifinality and induces uncertainties in the model calibration. As a result, taking into account additional observations in calibration could help for a better constraining of the model and in return a reduction of calibration uncertainties by reducing the number of acceptable parameter values [7]–[9]. Spatially distributed data about a flood event (e.g. water levels) would certainly help to reduce calibration uncertainties [10], but are very difficult to gauge in the field especially due to the risk of people being injured. A rather simple alternative way to obtain such distributed data is satellite imagery [11].

In this context, the aim of this study was to develop a methodology to obtain spatially distributed water levels using satellite SAR images and to integrate the estimates derived by remote sensing in hydraulic model calibration in an attempt to reduce model uncertainties. This extension of the calibration is done to show that the integration of RSD data could help to better constrain the model and thus make it more reliable for forecasting.

Based on the study of [12] that provides $\pm$ 20 cm average uncertainty using aerial photographs, the water level estimation method employed here is composed of three steps [13]: i) extraction of the flood extent limits which are relevant for water level estimation, ii) initial estimation of water levels by merging the relevant limits and a high resolution high

R. Hostache, G. Schumann, P. Matgen, L. Hoffmann and L. Pfister are with the Public Research Center-Gabriel Lippmann (EVA Department), L4422 Belvaux, Grand-Duchy of Luxembourg.

G. Schumann is with the School of Geographical Sciences, University of Bristol, BS8 1SS, Bristol, UK, as Visiting Research Fellow

C. Puech is with the Cemagref (TETIS Research Unit), F-34093 Montpellier, France.

Manuscript received ; revised .

accuracy Digital Elevation Model (DEM), iii) minimization of estimation uncertainties of remotely sensed water levels by the introduction of hydraulic coherence concepts. To show the potential of satellite images for model uncertainty reduction, a stepped calibration approach has been adopted. In a first step, a traditional calibration is done using a recorded hydrograph. In a second step, the calibration is improved by the integration of RSD water levels.

II. Study area and available data

The area of interest includes a 18 km reach of the River Alzette (Grand-Duchy of Luxembourg) between Pfaffenthal and Mersch. In this area, the River Alzette meanders in a flat plain that has an average width of 300 m and a mean slope of 0.08 %. The average channel depth is 4 m. At Mersch, the drainage area of the river Alzette covers 404 km^2. This represents 34 % of the total area of the Alzette catchment. Although some large villages lie within the natural floodplain of the river, no severe damages were recorded for the early January 2003 flood [11], which had a peak discharge of around 70.5 $m^3.s^{-1}$ at the Pfaffenthal hydrometric station, corresponding to a return period of 5 years. With approximately 3 $km.h^{-1}$, the velocity of the flood peak propagation in the Alzette plain is low.

The image used in this study has been acquired by the Synthetic Aperture Radar (SAR) sensor of the ENVISAT satellite (descending orbit, C band ($5.6cm$ wavelength), Vertical-Vertical (VV) and Vertical-Horizontal (VH) cross polarization) at 9:57 PM, on January 2^{nd} 2003, just after the flood peak, at the beginning of the recession. This radar image, amplitude coded, has a pixel spacing of 12.5 m, resulting from the sampling of a complex image of 25 m spatial resolution. The ENVISAT image has been georeferenced using Ground Control Points (GCP) on aerial photographs (digitized using a Geographic Information System). The RMSE after this georeferencing was 10 m. On C band radar images, smooth open water appears with a very low backscatter, due to a specular reflection. This allows a relatively straightforward detection of flooded areas [14]. However, wind and strong precipitations induce wavelets on the water surface and this may cause a roughening of the water surface, thereby increasing the backscatter [15]. This may occur for the SAR sensor of ENVISAT, especially if these wavelets have high vertical dimensions with respect to the incident signal wavelength [16]. At the image acquisition time, the wind speed was moderate (5 $m.s^{-1}$ recorded in a meteorologic station close to the study area), causing presumably negligible wind effects on open water surface roughness.

The collected hydrometric data are six limnigraphs that were recorded at the stream gauges located in the villages of Pfaffenthal (Upstream), Walferdange, Steinsel, Hunsdorf, Lintgen and Mersch (Downstream), plotted in Fig. 2. As shown in this figure the limnigraphs of Lintgen and Hunsdorf are only available for low water depth because of measurement system disability. Moreover, the coordinates (X,Y) of 84 high water marks have been measured on the ground with a GPS ($\approx$ 5 m planimetric accuracy) and the maximum water level

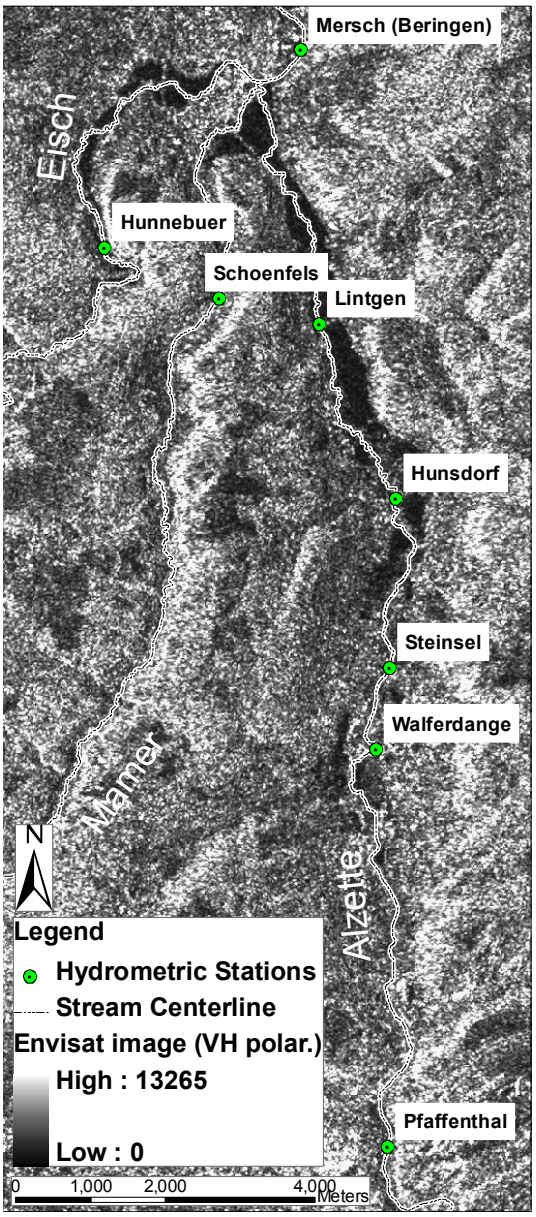

Fig. 1. Study area, Envisat SAR image (VH polarization) and hydrometric stations.

during the flood event has been measured using a theodolite (altimetric accuracy around $\pm$ 2 cm) at 7 points distributed across the floodplain.

The altimetric data used in this study are:

- a LiDAR DEM with a 2 m spatial resolution and a $\pm$ 15 cm mean altimetric uncertainty, for the floodplain terrain elevations,
- 200 bathymetric cross sections with a "theoretical" (some errors of more than 30 cm have been found during ground control survey) centimetric altimetric uncertainty, for the river channel elevations.

III. Methods

The methodology presented in this study aims at estimating spatially distributed water levels from remote sensing observations. Moreover, the approach that is used in this paper

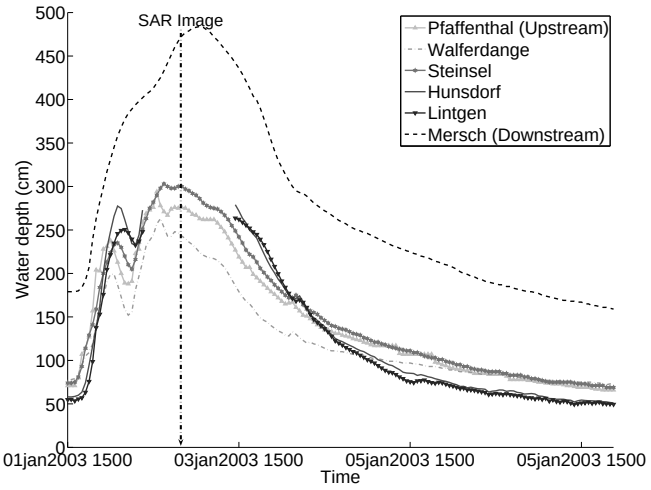

Fig. 2. Limnigraphs recorded and SAR image acquisition time.

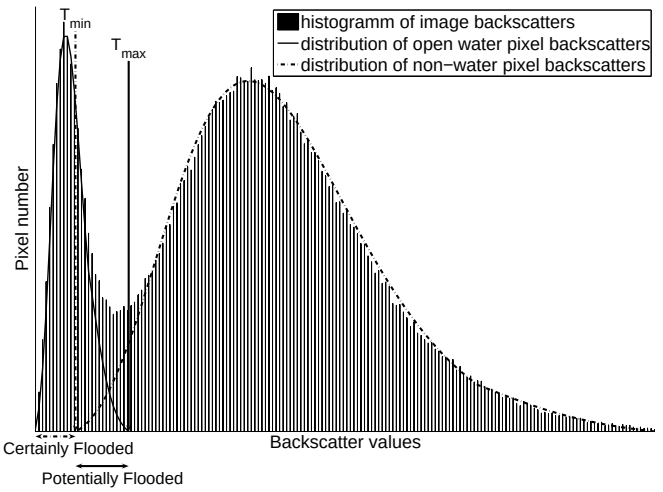

Fig. 3. Illustration of the overlapping of the water bodies and other land use types radiometric distributions on the histogram of a flood SAR image and proposed values of the two thresholds used for flood extent mapping

aims at integrating the remote sensing derived information in a hydraulic model in order to reduce model uncertainties.

A. Water level estimation

1) Extraction of the flood extent limits that are relevant for water level estimation: Flood extent mapping using SAR images is widely applied [2] because water appears with very low backscatter compared to other objects, thereby making flooded area detection relatively straightforward. In this study, radiometric thresholding has been used because it is a robust and reliable way [14] to detect flooded areas on SAR images. On the image, the radiometric distributions of water bodies and other land use types are not totally separated and do thus overlay (see Fig. 3). As a result it is very difficult to find a single threshold value that permits to detect water bodies only. To deal with this radiometric uncertainty, two thresholds are applied (see Fig. 3). The first one, T_{min}, aims at detecting only pixels that correspond to water bodies. As a matter of fact, T_{min} represents the minimum radiometric value of non-flooded pixels (e.g. outside the floodplain and outside the permanent water surfaces). Then all pixels with a lower backscatter than T_{min} only correspond to water. Considering that the backscatter of grassland is one of the lowest in the SAR image except water, the proposed value for T_{min} is the minimum radiometric value of grassland outside the flooded area. The second one, T_{max}, aims at detecting all flooded areas, at the risk of detecting in addition non-flooded areas that have a similar radiometric value to the flooded one. The proposed value for T_{max} is the maximum radiometric value of water bodies outside the flooded area (e.g. lakes or the river channel if wide enough). Using these two thresholds, it is possible to obtain a flood extent map with three values: 0 = non-flooded ($image \quad radiometry > T_{max}$), 1 = certainly flooded ($image \quad radiometry < T_{min}$), 2 = potentially flooded ($T_{min} \leq image \quad radiometry \leq T_{max}$). Then, except in case of local errors in the flood extent map that will be treated thereafter, pixels equal to 1 correspond only to open water and pixels equal to 0 correspond only to non open water. This induces that the potentially flooded areas (pixels equal to 2) define fuzzy limits of the flooded areas that take into account radiometric uncertainty, given that two thresholds have been applied to the SAR image. Moreover, the accuracy of the georeferencing of a SAR image induces additional uncertainties on these fuzzy limits that need to be taken into account. To do this, it has been chosen to buffer the fuzzy limits with a size equal to the SAR image georeferencing accuracy (10 m for the ENVISAT image). These buffered fuzzy limits that take into account radiometric and spatial uncertainties from the SAR image will be used for water level estimation.

The innovative part of the SAR image processing is to analyze the relevance of the flood extent map for hydraulic purposes, and especially for water level estimation. To derive water levels, the method is based on the merge between the most trustworthy limits of the flood extent map and the underlying DEM, as proposed by [17]. Considering that both buildings and high vegetation may mask water on a SAR image [18], the corresponding areas are considered as being irrelevant since they may cause artificial flood extent limits, and thus produce wrong water level estimates. As a consequence, the removal of building and high vegetation areas from the flood extension map analysis allows to retain only areas that are correctly allocated to either flooded or non-flooded for the water level estimation. Moreover, due to spatial and radiometric uncertainties resulting from the SAR image and its processing, the extracted flood extension limits are always prone to uncertainty. As a matter of fact, during the merging between the flood extension limits and the DEM, this uncertainty is transferred to the water level estimates [17], [19]. Consequently, areas with gentle relief have been considered irrelevant for water level estimation because they imply important uncertainties on water level estimates. After the removal of irrelevant parts of the remotely sensed flood extent limits, only the most reliable limits remain. These are shaped as small patches that are sparsely distributed across the

floodplain.

2) Initial water level estimation: Considering that radiometric and spatial uncertainties have been taken into account using two thresholds and a buffering and that error prone areas on the flood extent map (i.e. residential and vegetated areas that mask water) have been removed beforehand, the remaining relevant limits are assumed to include the real flood extent limits (*Hyp. 1*). Under this hypothetis, the merging of relevant limits and the DEM allows the extraction of the terrain elevations inside all relevant limits and thus an estimation of intervals of water levels that should include the true value, provided that the DEM altimetric uncertainty ($uncert_{DEM}$) is taken into account. To take the DEM altimetric uncertainty into account, it has been chosen to enlarge the intervals of water level estimation using the DEM altimetric uncertainty ($uncert_{DEM} = \pm 15\ cm$ for the LiDAR DEM of the study area): if $El^{sat}_{min,i}$ and $El^{sat}_{max,i}$ are respectively the minimum and the maximum values of the terrain elevation inside a given relevant limits, then, the interval of water level estimation will be $IWL^{sat}_i = [WL^{sat}_{min,i}; WL^{sat}_{max,i}] = [El^{sat}_{min,i} - uncert_{DEM}; El^{sat}_{max,i} + uncert_{DEM}]$. Then each resulting interval of water level estimation - IWL^{sat}_i - is assumed to include the real local water level (*Hyp. 2*). However, these estimation intervals are independent, resulting from a remote sensing process, without considering hydraulic laws governing water flow. Consequently, the water level estimation method is enhanced by a hydraulic coherence algorithm, previously developed by [12] for water levels estimated from aerial photographs.

3) Constraining of initial water level estimates using hydraulic coherence concepts: The hydraulic coherence algorithm is based on the law stating that hydraulic energy decreases from upstream to downstream. Under the assumption of low flow velocity, which is acceptable in the Alzette floodplain, this hydraulic law can be simplified into a decrease of water level in the flow direction (*Hyp. 3*). To apply *Hyp. 3* to the remotely sensed water levels IWL^{sat}, the flow directions between locations of water level estimates need to be known. For hydraulic modeling, a one-dimensional (1D) model has been developed. This model is based on the assumption of 1D hydraulic flow. This means that the water flows from one cross section to the following starting at the first cross section (upstream boundary condition) and ending at the last one (downstream boundary condition) [20]. Using the same assumption on the flow direction to the relevant limits, it has been possible to determine a hydraulic hierarchy, composed of up-/downstream relationships between locations of water level estimation - corresponding to the locations of the relevant limits. Thus, *Hyp. 3* means that if the relevant limit A is upstream of the relevant limit B, then the water level must decrease from A to B. Due to *Hyp. 2*, the hydraulic coherence algorithm may force the following constraints: $WL^{sat}_{max}(B) \leq WL^{sat}_{max}(A)$, and vice-versa $WL^{sat}_{min}(A) \geq WL^{sat}_{min}(B)$. As a consequence, propagating these constraints following the flow direction, the algorithm forces a decrease upon the maxima ($WL^{sat}_{max,i}$) from upstream to downstream and a rising upon the minima ($WL^{sat}_{min,i}$) from downstream to upstream -see Fig. 4. This provides constrained water level estimates, called final water levels hereafter, that will be integrated in the calibration process.

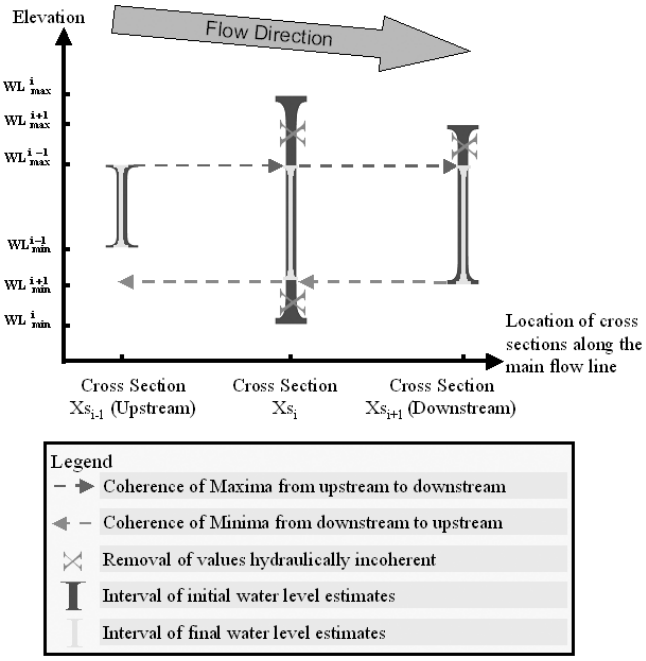

Fig. 4. Propagation scheme of the hydraulic coherence constraints on initial water level estimates.

B. Reduction of hydraulic model calibration uncertainty using remote sensing derived water levels

The aim of the second part of the methodology is to better constrain the hydrodynamic model using the RSD spatially distributed water levels resulting from the previous treatments. Some previous studies (e.g. [7], [8], [21]) have shown that flood extents derived from SAR images could be useful for hydraulic model calibration. The originality in this study is to integrate a different kind of information derived from SAR, namely water levels. To emphasize the integration of such remote sensing derived data sets in addition to traditional calibration data, e.g. hydrographs, a two-step approach is adopted. The first step of the calibration procedure refers only to point measurements in the form of a hydrograph as reference data. In the second step, the remotely sensed water levels are integrated to enhance the calibration and better constrain the hydraulic model. To deal with uncertainties of the observed data and the parameter value determination, the calibration process has been inspired by the GLUE methodology [6], based on Monte-Carlo simulations.

1) Hydraulic model and parameters: The set up of a hydraulic model requires the knowledge of a three-dimensional (3D) geometry of the floodplain and channel, initial conditions, boundary conditions and hydraulic parameters, e.g. friction coefficients. For a one dimensional (1D) hydraulic model, the geometry is defined by a main flow line - usually the median axis of the river channel [20], and cross sections, placed perpendicularly to the main flow line (Fig. 5). In 1D modeling, it is assumed that the water level is uniform on each

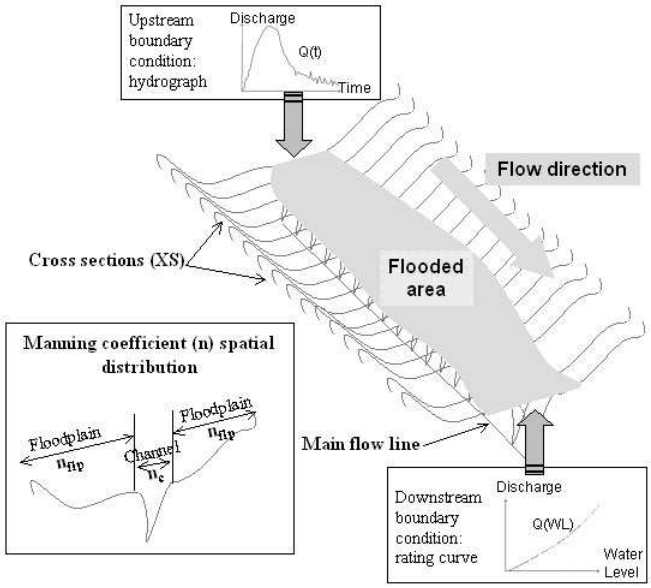

Fig. 5. One-Dimensionnal model geometry and Manning's friction coefficients.

cross section. The hydraulic model used in this study has been set up under Hec-RAS [22]. The 3D geometry of the model has been extracted using the DEM and the bathymetric data (Cf. section II). The boundary conditions (Fig. 5) of the model are as follows:

- upstream boundary condition: the hydrograph calculated at the Pfaffenthal (Fig. 1 and 2) hydrometric station using the recorded limnigraphs and a rating curve (relationship between water depth and discharge),
- downstream boundary condition: the rating curve at the Mersch hydrometric station.

Furthermore, two tributaries -Rivers Eisch and Mamer- have their confluences with the river Alzette between two cross sections of the hydraulic model geometry, upstream of Mersch City. As a consequence, a hydrograph for these two tributaries has been calculated using the rating curves and the limnigraphs recorded at Schoenfels (River Mamer) and Hunnebuer (River Eisch) stream gauges (Fig. 1). The initial condition is calculated by the model as a steady flow simulation using the discharge at the Pfaffenthal hydrometric station (upstream boundary) at the starting time. The calibration parameters are two Manning friction coefficients (one for the river channel and one for the floodplain, see Fig. 5). A single channel Manning coefficient has been attributed for the entire reach in the model because the channel aspect appeared homogeneous along the study area during field observations [21]. Moreover, the aim is to avoid over-parameterization and to focus on the interest of taking remotely sensed water level into account during calibration. Besides, with friction inside the floodplain being higher than inside the riverbed, the Manning coefficient in the floodplain should be higher than that of the channel.

2) Calibration process: The aim of a calibration is to find the parameter values that enable the model to provide outputs that are as close as possible to observations. If no satisfactory results can be obtained with any of the tested parameter sets, the model assumptions, the model structure and the boundary conditions should be questioned [6]. The calibration process used in this study is based on a random generation of parameter sets and subsequent hydraulic model simulations with each set of parameters. Next, outputs provided by each simulation are compared to recorded observations. Using this kind of calibration process, it is possible to represent performances of the model versus parameter values [8]. In the first calibration step, applying the widely used Nash criterion [23] (1) to assess model performance, the simulated hydrograph at the downstream cross section is compared to the hydrograph estimated using the rating curve and the recorded water levels at the Mersch hydrometric station.

$$C_{Nash} = 1 - \sqrt{\frac{\sum_{t=t_0}^{t_{end}} \left(Q_{sim}(t) - Q_{obs}(t)\right)^2}{\sum_{t=t_0}^{t_{end}} \left(Q_{sim}(t) - \overline{Q_{obs}}\right)^2}} \tag{1}$$

In (1), $Q_{obs}(t)$ and $Q_{sim}(t)$ are respectively the observed and simulated discharges at time t, t_0 and t_{end} are the starting and ending time of the simulations, $\overline{Q_{obs}}$ is the average observed discharge between t_0 and t_{end}. The Nash criterion represents the percentage of the observed discharge variance explained by the model. The Nash criterion is equal to 1 if the observed and simulated hydrographs fit perfectly and the more divergent these hydrographs, the lower the Nash criterion. A value of the Nash Criterion lower than 0 means that the model provides worse results than the average observed discharge $\overline{Q_{obs}}$. The Nash criterion is well suitable for a flood model evaluation, since it gives more weight to the highest values of discharge in the performance calculation.

In the second calibration step the model outputs are also compared to the RSD water levels. Each simulation is stopped at the timestep t_{sat} of the satellite overpass and the performance is calculated using simulated and RSD water levels. The criterion chosen to evaluate the model performance is given in (2).

$$C_{sat} = \sum_{i=1}^{N} \left(\frac{\Delta WL_i}{N}\right)$$
$$\text{with: } \Delta WL_i = \left\{ \begin{array}{l} 1 \text{ if } WL_{i,t_{sat}}^{sim} \in IWL_i^{sat} \\ 0 \text{ if } WL_{i,t_{sat}}^{sim} \notin IWL_i^{sat} \end{array} \right\} \tag{2}$$

In (2), $WL_{i,t_{sat}}^{sim}$ is the simulated water level at the satellite flyover time, $IWL_i^{sat} = [WL_{min,i}^{sat}; WL_{max,i}^{sat}]$ is the interval of the RSD water level on the model cross section i, and N is the number of model cross sections where a RSD water level is available. This performance criterion provides a percentage value of cross sections (between 0 and 1) where the simulated water level is included in the corresponding interval of the RSD water level. It is equal to 1 if the simulated water levels are inside the intervals of RSD water levels everywhere.

IV. Results and Discussion

The following subsections outline the findings of this study and discuss their implications.

A. Water level estimation

The first step of the water level estimation method is the extraction of the flood extent using the SAR image. To extract the flood extent, a double thresholding (on each polarization) has been applied to the georeferenced ENVISAT image (Fig. 6). Considering that the backscatter of grassland is one of the lowest in the SAR image except water, the threshold values have been calculated, for each polarization, using the maximum intensity of permanent water (lakes) for T_{max} and the minimum values of grassland for T_{min} (estimated thanks to spatial statistics using a GIS). The thresholding of the SAR image using T_{min} and T_{max} provide the flood extent map shown in Fig. 6.

As described in section III-A1, the fuzzy limits of the flood extent (pixels equal to "2": potentially flooded) have been buffered using a 10 m distance in order to take into account spatial uncertainty linked to the SAR image georeferencing. Then, considering that the spatial and radiometric uncertainties have been taken into account in the buffered fuzzy limits, *Hyp. 1* is applied, i.e. it can be assumed that the real limit of the flooded area is located inside these fuzzy limits except for emerging objects that mask water -e.g. trees and buildings. The presence of trees or buildings inside the flooded area create "artificial" holes inside the flood extent map and thus flood boundaries that do not necessarily match the "true" flood extent limits. With the water level estimation method proposed in section III-A2 based on a merging between flood extent limits and a DEM, any error on these limits will induce errors in the water level estimates. Moreover, as mentioned in section III-A1, flood extent limits located on areas with gentle relief are irrelevant for water level estimation because they lead to large uncertainties. As a result, the limits of the flood extent map located in areas with gentle relief, trees and buildings were removed for an accurate water level estimation.

As partial validation of the RSD flood boundaries, ground surveyed high water marks (light dots) located in areas without trees or buildings have been added to Fig. 6. 92 % of these are included in the fuzzy limits of the flood extent map. Moreover, the mean distance between the high water marks that lie outside the fuzzy limits and these fuzzy limits is equal to $4\ m$. This is lower than the coordinate accuracy of these points (accuracy of the GPS used to calculate the high water marks is of approximately $5\ m$). As a consequence, these results show that the method employed in this study for flood extent mapping is suitable. Hence, the *Hyp. 1* and the assumption of low wind effects on water surface roughness are appropriate.

After the removal of areas that are irrelevant for water level estimation, the remaining limits of the flood extent map, merged with the LiDAR DEM, allow an initial water level estimation as shown in Fig. 7 (a). As the limits of the flood extent map are fuzzy, the resulting water level estimates are in the form of intervals. In Fig. 7 (a), the boundaries (resp. $WL_{min,i}$ and $WL_{max,i}$) of each interval of water level estimation (resp. black diamonds and black squares), are plotted against their location in the floodplain from upstream to downstream (descending abscissa along the main flow line of the hydraulic model geometry). As reference data, the field surveyed high water marks (grey dots) and the river channel bottom elevation (black line) have been added.

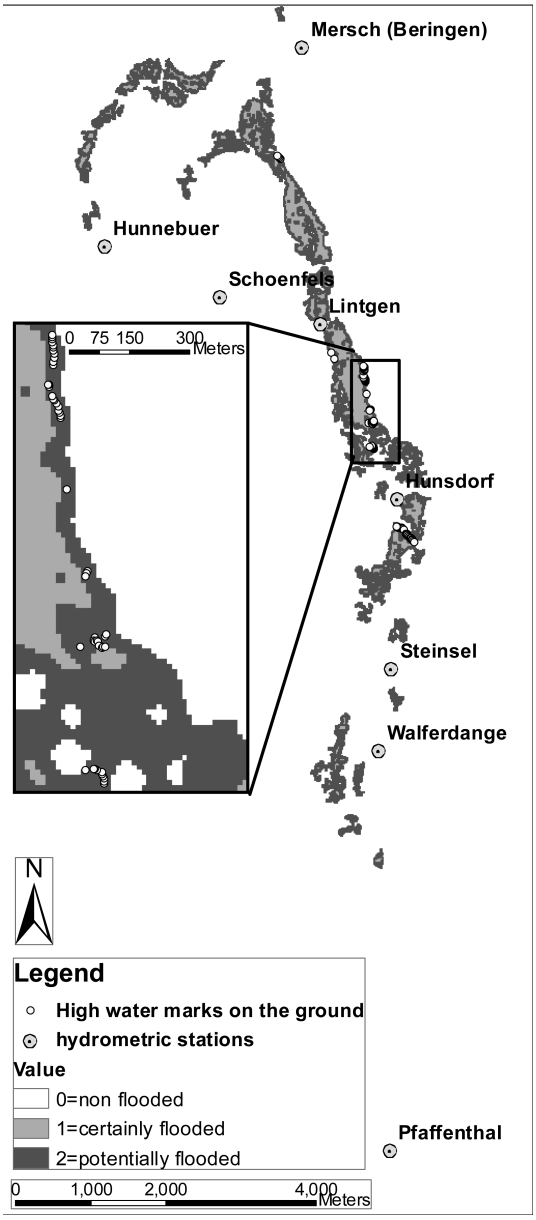

Fig. 6. SAR image derived flood extent map.

To characterize the uncertainty of the resulting initial water level estimates, the half mean interval $\frac{mean(WL_{max}-WL_{min})}{2} = 88\ cm$ of the resulting water level estimates has been calculated. This "mean uncertainty" of $\pm\ 88\ cm$, on the RSD water levels is relatively high and may be too large for hydraulic model constraining. Furthermore, these initial RSD water levels have been obtained only by remote sensing and spatial analysis, i.e. without considering physical laws governing a river flow.

Thus, as proposed in section III-A1, the constraining algorithm of initial water level estimates using hydraulic coherence concepts has been applied. These provide final water level estimates shown in Fig. 7 (b) with a mean uncertainty (see above) of $\pm\ 54\ cm$. Compared to the mean uncertainty of

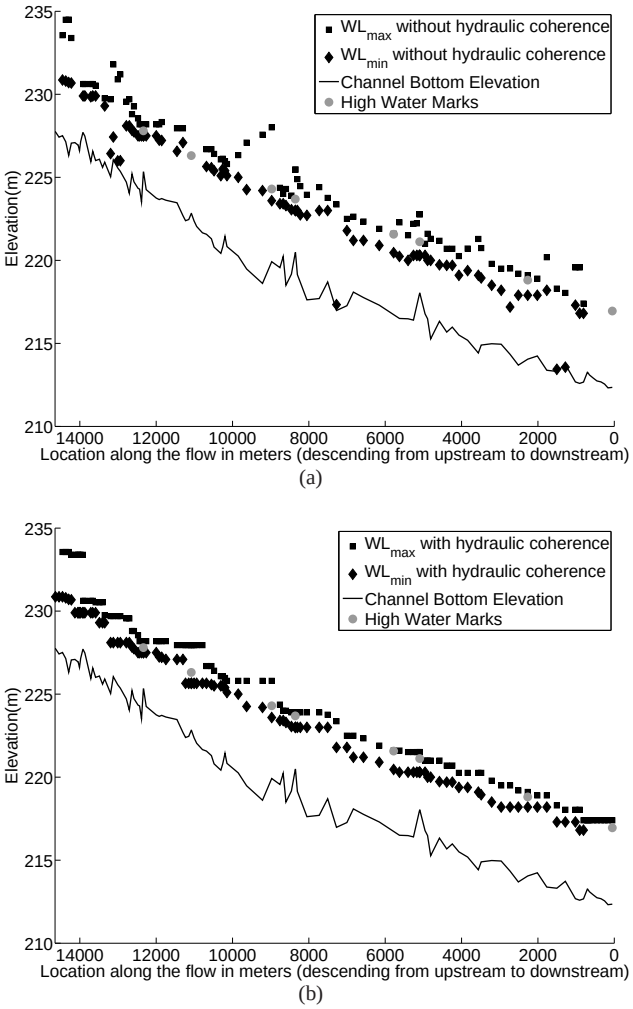

Fig. 7. Remote sensing derived water levels before (a) and after (b) the hydraulic coherence constrain.

the initial RSD water levels ($\pm$ 88 cm), this value shows a significant improvement and let one expect a better capability of the final water levels to constrain the hydraulic model. Given that the mean value ($\frac{WL_{min}+WL_{max}}{2}$) of each RSD water level interval represents a single estimate of the water level, a RMSE of 30 cm between these single estimates and the high water marks measured in the field has been calculated. Although this RMSE is not an absolute measurement of the RSD water level accuracy, it shows that the water level estimation method presented in this study provides results that might be usable for hydraulic modeling.

Moreover, the Fig. 7 (b), shows that each *in situ* high water marks measurement is included in the corresponding interval of RSD water level, which is crucial because it validates at least partially the RSD water levels and especially *Hyp. 2* which states that the "true" water level is inside the intervals of RSD water levels.

B. Reduction of hydraulic model calibration uncertainty using remote sensing derived water levels

As proposed in section III-B2, the calibration of the hydraulic model was based on Monte-Carlo simulations. For this

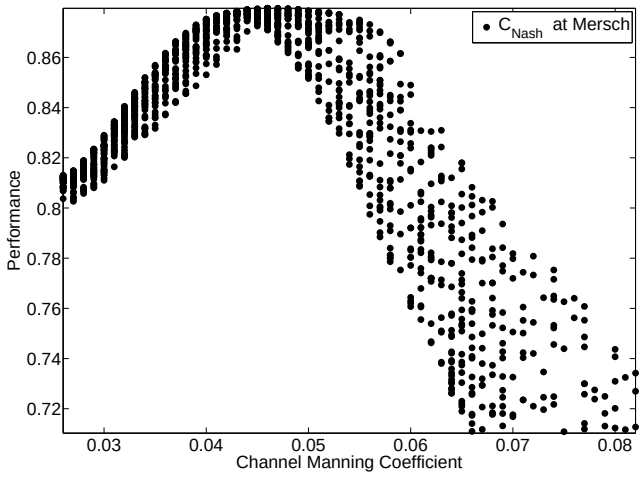

Fig. 8. Evaluation of the model results using the Nash criterion (1) for the downstream cross section of the model (Mersch hydrometric station)

procedure, 2000 sets of parameters were randomly generated within the following intervals of physically plausible values:

- for the channel Manning coefficient: $n_c \in [0.01; 0.1]$
- for the floodplain Manning coefficient: $n_{flp} \in [0.01; 0.2]$

Next, for each generated set of parameters, one hydraulic model run (between the 1^{st} of January 2003, at 03:00 PM, and the 8^{th} of January 2003, at 00:00 AM) was performed, and the results of these simulations were compared with observations. To underline the effects of the integration of RSD water levels on model calibration uncertainties, the evaluation of the results has been carried out in two steps.

The first step is a comparison between simulated and observed hydrographs at the downstream boundary of the model. The performance criterion used for this comparison is the Nash criterion (1). Fig. 8 shows the dotty plot resulting from the calculation of the Nash criterion. On this figure, each dot corresponds to the evaluation of the model result for one set of parameters (one single value for both the channel and the floodplain Manning coefficient). The higher the Nash criterion, the better the match between the simulated and the observed hydrograph. It is worth noting that in Fig. 8, the Nash criterion has not been plotted versus the floodplain Manning coefficient, as no sensitivity was obvious for the 2003 flood event. A simple reason is that this flood event is of relatively low magnitude (5 year return period), which induces that most of the water (more than 90 % in this case) flows through the channel.

As a perfect fit between model results and observations is impossible due to unavoidable model errors, it is reasonable to consider a Nash criterion higher than 0.85 as an acceptable model performance. Indeed, as argued by [10], when considering a too high value as acceptable for a performance criterion there is a risk to consider not a single model as acceptable. As a matter of fact, it is found that the acceptable values of parameters are within the following intervals:

- for the channel Manning coefficient: $n_c \in [0.036; 0.059]$
- for the floodplain Manning coefficient:

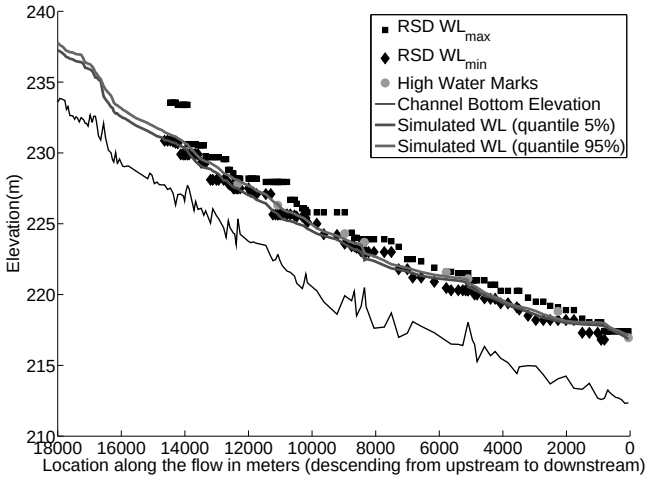

Fig. 9. Quantiles (5 % and 95 %) of the water lines simulated by the hydraulic model "calibrated" using only the Nash criterion, in comparison to high water marks and RSD water levels

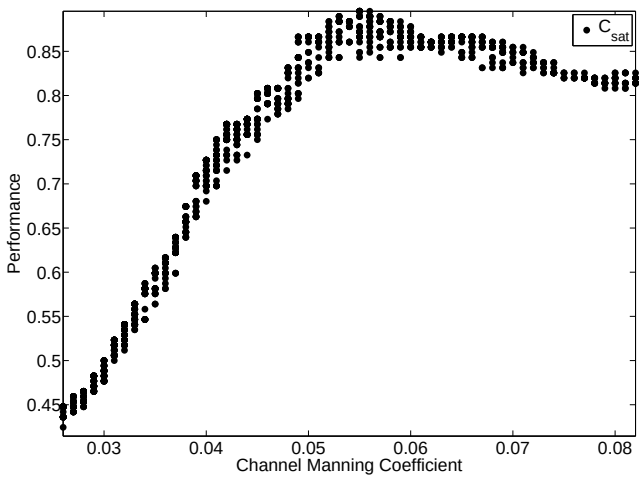

Fig. 10. Evaluation of the model results using the criterion (2) based on the remote sensing derived water levels

$$n_{flp} \in [0.044; 0.2]$$

Fig. 9 presents the 5 % and 95 % quantiles of the water lines simulated using the acceptable parameter sets. Between these two water lines, the mean water level deviation is equal to 43 cm. This value is an indicator of the model calibation uncertainty, but does not provide the predictive accuracy and reliability of the model results. To assess this accuracy, the methodology that has been chosen in this article is the calculation of an RMSE between the 50 % quantile of the simulated water lines and all ground measurements of water level. These include six limnigraphs and seven high water marks (see section II). Then, this RMSE calculation provides an average accuracy of the acceptable models in the order of 28 cm. Hence, these results show that the uncertainty on the model results could be important if the calibration is only done using point measurements, even if they are distributed in time. As a consequence, the second step of the calibration process was to integrate, in addition to a downstream hydrograph, the RSD water levels for a better constraining of the model and thereby a reduction of the calibration uncertainties.

The performance criterion used to evaluate the model results when comparing simulated with RSD water levels is given in (2). The dotty plot that arises from this evaluation is presented in Fig. 10. Then, considering that a Nash (C_{Nash}) and a satellite based (C_{Sat}) criteria higher than 0.85 provide acceptable models, the acceptable parameter values lie within the following intervals: $n_c \in [0.049; 0.056]$ and $n_{flp} \in [0.063; 0.179]$. As a consequence the resulting ensembles of acceptable parameters are more restricted than in the case of an evaluation based only on hydrographs. This means that RSD observations allowed the rejection of some Manning coefficient values that are acceptable according to the downstream hydrograph, but that do not provide satisfactory results in terms of spatially distributed water levels. Furthermore, although the acceptable values of the channel Manning coefficient seem higher than those expected for such a river, the ensembles of acceptable parameters obtained in this study are in agreement with those obtained by [21] for a similar reach of the river Alzette. Fig. 11 shows the 5 % and 95 % quantiles of the water lines simulated by the acceptable hydraulic models with respect to both downstream hydrograph and RSD water levels data sets. The mean water level deviation between these two water lines is 13 cm, which shows a significant reduction of the model calibation uncertainty. Moreover, the RMSE calculated between the 50 % quantile of the simulated water lines and the field measurements is equal to 25 cm. As a matter of fact, the integration of the RSD water levels in the calibration process, in addition to the donwstream hydrograph, allowed a better constraining of the model and thus renders its results less uncertain and more reliable.

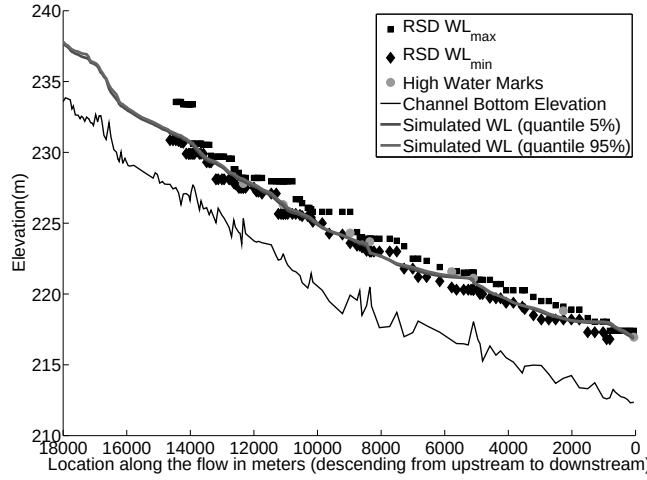

Fig. 11. Quantiles (5 % and 95 %) of the water lines simulated by the hydraulic model "calibrated" using both the Nash and satellite based criteria, in comparison to high water marks and RSD water levels

As proposed in section III-A3, the RSD water levels have been obtained thanks to a constraining of the initial water levels using hydraulic coherence concepts. To show the effect of such a constraining on the capability of RSD water levels to reduce hydraulic model calibration uncertainties, the calibration process presented above has been applied using the

downstream hydograph and the intial RSD water levels. In this case, with acceptable Nash (C_{Nash}) and satellite-based (C_{Sat}) criteria higher than 0.85, the acceptable values of parameters lie within the following intervals:$n_c \in [0.045; 0.059]$ and $n_{flp} \in [0.051; 0.2]$ The mean water level deviation between the $5\ \%$ and $95\ \%$ quantiles of the simulated water lines is $25\ cm$, which shows a reduction of the model calibation uncertainty that is significantly lower than in the case of the calibration done using final RSD water levels. This proofs that the hydraulic coherence algorithm is a tool of the water level estimation method that significantly enhances the capability of the RSD water levels to reduce uncertainties in the hydraulic model calibration.

As validation of the "calibrated" model for the 2003 flood event when using the downstream hydrograph and the final RSD water levels, hydraulic simulations have been performed for the 2007 flood event (between the 17^{th} of January 2007, at 00:00 AM, and the 21^{th} of January 2007, at 00:00 AM). For this flood event, limnigraphs for the Pfaffenthal (Upstream), Walferdange, Steinsel, Hunsdorf, Lintgen and Mersch (Downstream) stream gauges were available. The boundary conditions used for these simulation are:

- upstream boundary condition: the hydrograph calculated at the Pfaffenthal hydrometric station using the recorded limnigraph and a rating curve,
- downstream boundary condition: the rating curve at the Mersch hydrometric station.

A comparison of the six observed limnigraphs with the $50\ \%$ quantile of the corresponding simulated limnigraphs gave an RMSE value of $22\ cm$, which is in the same order of magnitude than the RMSE calculated for the 2003 flood event. This RMSE can be considered as acceptable, and indicates that the model is reliable for forecasting.

V. Conclusion

[2] argues that data that can be extracted from a SAR flood image are not restricted to flood extents. In this context, a previous study [10] showed water level estimations with a mean uncertainty of 1-3 m, when merging SAR RSD flood extent limits with a DEM. Nevertheless, this uncertainty is too large for hydraulic modeling purposes. [11] show that it is possible to estimate water levels with an acceptable accuracy ($\approx \pm 18\ cm$) using both a high resolution-high accuracy DEM and a SAR image, but the REFIX method developped by [11] seems a bit less adapted for hydraulic model calibration because the uncertainty on the resulting RSD water levels may not be easily assessed [19]. Hence, the methodology presented in this study estimates water levels accurately enough for integration with hydraulic models to reduce uncertainties in model calibration. The RSD water level estimates have been obtained with a $\pm\ 54\ cm$ mean uncertainty, using an ENVISAT ASAR image of a River Alzette flood event. This water level estimation presents lower uncertainty than [17]. It has been conducted using an analysis of the relevance of RSD flood extent in terms of hydraulics and a merging between relevant limits and a DEM coupled with a hydraulic coherence algorithm developed by [12]. Although the uncertainty is higher in the current study than in [12], satellite imagery offers enhanced capability to obtain RSD water levels that are accurate enough to be useful in hydraulic model calibration. Integrated in a hydraulic model during calibration in addition to traditional calibration data -e.g. hydrographs-, these RSD water levels are capable of significantly reducing uncertainties - i.e. by reducing the ranges of acceptable parameter values. The predictions of the calibrated model become more suitable thanks to a better constraining, both temporally and spatially.

As a consequence, the methodology presents two main advantages. It provides distributed water levels with a high spatial density over large areas and provides more reliable hydraulic models thanks to these water levels that allow a spatial evaluation of model performances. Indeed, the simulated water level uncertainty decreases from $40\ cm$ to $13\ cm$ and the RMSE between simulated and observed water levels keep approximately the same value ($28\ cm$ to $25\ cm$) thanks to the integration of RSD water levels in the model calibration process. Moreover, using acceptable parameter sets obtained when using both field measurments of water levels and RSD water levels (2003 flood event), it has been possible to show that the model's accuracy in forecasting of the 2007 flood event has a magnitude in the order of $22\ cm$. This shows that the calibrated model using both hydrometric and RSD data is well constrained and reliable for forecasting.

With the launch of new radar satellites (e.g. RADARSAT-2, ALOS, Cosmo-Skymed, TerraSar-X) that have better spatial and radiometric resolutions, the uncertainties of water level estimates will presumably be further reduced, getting closer to the results of [12] obtained with aerial photographs. Moreover, in addition to the use of RSD water levels for calibration, it would be of great interest to evaluate the possibilities of assimilating such data in hydraulic models. This may allow the forecasting of flood extents with a higher accuracy after the acquisition of a satellite image.

Acknowledgment

This study has been partially funded by the National Research Fund (FNR) of Luxembourg through the VIVRE program (FNR/VIVRE/06/36/04), and the Belgian Science Policy Office in the framework of the STEREO II program - project SR/00/100.

References

[1] R. Oberstadler, H. Hönsch, and D. Huth, "Assessment of the mapping capabilities of ERS-1 SAR data for flood mapping: a case study in Germany," *Hydrological Processes*, vol. 11, no. 10, pp. 1415–1425, 1997.

[2] L. C. Smith, "Satellite remote sensing of river inundation area, stage and discharge : a review," *Hydrological Processes*, vol. 11, pp. 1427–1439, 1997.

[3] F. Pappenberger, K. Beven, M. Horritt, and S. Blazkova, "Uncertainty in the calibration of effective roughness parameters in HEC-RAS using inundation and downstream level observations," *Journal of Hydrology*, vol. 302, no. 1-4, pp. 46–69, 2005.

[4] M. S. Horritt and P. D. Bates, "Evaluation of 1D and 2D numerical models for predicting river flood inundation," *Journal of Hydrology*, vol. 268, no. 1-4, pp. 87–99, 2002.

[5] G. Aronica, B. Hankin, and K. Beven, "Uncertainty and equifinality in calibrating distributed roughness coefficients in a flood propagation model with limited data," *Advances in Water Resources*, vol. 22, pp. 349–365, 1998.

[6] K. Beven and A. Binley, "The future of distributed models - model calibration and uncertainty prediction," *Hydrological Processes*, vol. 6, no. 3, pp. 279–298, 1992.
[7] P. Matgen, J.-B. Henry, F. Pappenberger, P. de Fraipont, L. Hoffmann, and L. Pfister, "Uncertainty in calibrating flood propagation models with flood boundaries derived from synthetic aperture radar imagery," pp. 352–358, in: Proceedings of the 20th Congress of the International Society of Photogrammetry and Remote Sensing, Istambul, Turkey, 2004.
[8] M. S. Horritt, "Calibration of a two-dimensional finite element flood flow model using satellite radar imagery," *Water Resources Research*, vol. 36, no. 11, pp. 3279–3291, 2000.
[9] P. Bates, "Remote sensing and flood inundation modelling," *Hydrological Processes*, vol. 18, no. 13, pp. 2593–2597, 2004.
[10] G. Schumann, M. Cutler, A. Black, P. Matgen, L. Pfister, L. Hoffmann, and P. Florian Pappenberger, "Evaluating uncertain flood inundation predictions with uncertain remotely sensed water stages," *Journal of River Basin Management*, In Press.
[11] G. Schumann, R. Hostache, C. Puech, L. Hoffmann, P. Matgen, F. Pappenberger, and L. Pfister, "High-resolution 3D flood information from radar imagery for flood hazard management," *IEEE Transactions on Geoscience and Remote Sensing*, vol. 45, no. 6, pp. 1715–1725, 2007.
[12] D. Raclot and C. Puech, "What does AI contribute to hydrology? Aerial photos and flood levels," *Applied Artificial Intelligence*, vol. 17, no. 1, pp. 71–86, 2003.
[13] R. Hostache, C. Puech, G. Schumann, and P. Matgen, "Estimation of water levels in a floodplain with satellite radar images and fine topographic data (in french : Estimation de niveaux d'eau en plaine inondée à partir d'images satellites radar et de données topographiques fines)," *Remote Sensing Journal (In French: Revue Télédétection)*, vol. 6, no. 4, pp. 325–343, 2006.
[14] J.-B. Henry, "Spatial information system for floodplain inundation risk management (in french : Systèmes d'information spatiaux pour la gestion du risque d'inondation de plaine)," Ph.D. dissertation, Strasbourg I University, France, 2004.
[15] Z. Liu, F. Huang, L. Li, and E. Wan, "Dynamic monitoring and damage evaluation of floods in north-west Jilin with remote sensing," *International Journal of Remote Sensing*, vol. 23, no. 18, pp. 3669–3679, 2002.
[16] F. Ulaby and M. Dobson, *Handbook of radar scattering statistics for terrain*. Norwood (MA, USA): Artech House, 1989.
[17] G. R. Brakenridge, B. T. Tracy, and J. C. Knox, "Orbital SAR remote sensing of a river flood wave," *International Journal of Remote Sensing*, vol. 19, no. 7, pp. 1439–1445, 1998.
[18] M. S. Horritt, D. C. Mason, and A. J. Luckman, "Flood boundary delineation from synthetic aperture radar imagery using a statistical active contour model," *International Journal of Remote Sensing*, vol. 22, no. 13, pp. 2489–2507, 2001.
[19] G. Schumann, F. Pappenberger, and L. Matgen, "Estimating uncertainty associated with water stages from a single sar image using a stepped glue approach," *Advances in Water Resources*, submitted.
[20] H. Roux and D. Dartus, "Use of parameter optimization to estimate a flood wave: Potential applications to remote sensing of rivers," *Journal of Hydrology*, vol. 328, no. 1-2, pp. 258–266, 2006.
[21] G. Schumann, L. Matgen, L. Hoffmann, R. Hostache, F. Pappenberger, and L. Pfister, "Deriving distributed roughness values from satellite radar data for flood inundation modelling," *Journal of Hydrology*, vol. 344, pp. 96–111, 2007.
[22] United States Army Corps of Engineers (USACE), "Theoretical basis for one-dimensional flow calculations," in *Hydraulic reference manual*. Davis (CA, USA): USACE, 2002, ch. 2, version 3.1. [Online]. Available: http://www.hec.usace.army.mil/software/hec-ras/
[23] J. E. Nash and J. V. Sutcliffe, "River flow forecasting through conceptual models. part 1: A discussion of principles," *Journal of Hydrology*, vol. 10, no. 3, pp. 282–290, 1970.